

Sigma Photoproduction from  $\text{CH}_2^\dagger$ 

CHARLES E. ROOS

*Vanderbilt University, Nashville, Tennessee*

AND

V. Z. PETERSON\*

*California Institute of Technology, Pasadena, California*

(Received 26 March 1964)

The first photoproduced sigmas have been observed by placing nuclear emulsions within a few mm of a  $\text{CH}_2$  target. One dozen in-flight decays (10  $\Sigma^+$ 's and 2  $\Lambda^0$ 's) have been identified. The background which previously would have prevented useful exposures has been sharply reduced by applying a 160 KG field along the photon beam. The bulk of the electrons are held in small orbits while the heavier charged sigmas are relatively unaffected. Both of the sigma decay modes have been observed, as well as the charged mode for  $\Lambda^0$  decay. The sign of the charged-pion sigma decays cannot be distinguished. The sigma proton decay can only come from the  $\Sigma^+$  and this experiment provides the first measurement of the reaction,  $\gamma + p \rightarrow \Sigma^+ + K^0$ . No event has been included with less than 10% difference in ionization between primary and secondary. All observed events had at least one track with ionization greater than  $2\times$  minimum. If one corrects for the assumed loss of lighter events, the average cross section for photon energies between 1100 and 1200 MeV and for kaon c.m. angles between  $30^\circ$  and  $120^\circ$  ( $\sim 60^\circ$  c.m.) in  $\gamma + p \rightarrow \Sigma^+ + K^0$  is  $(4 \pm 2) \times 10^{-31} \text{ cm}^2/\text{sr}$ .

## INTRODUCTION

HYPERON photoreactions have been investigated by the observation of in-flight decays of the hyperons in nuclear emulsion. The detection<sup>1</sup> of a  $\Sigma^+$  provides the first measure of the reaction in Eq. (1).

$$\gamma + p \rightarrow \Sigma^+ + K^0. \quad (1)$$

Previous information<sup>2-4</sup> on hyperon photoprocesses was restricted to the three reactions which produce a charged kaon.

$$\gamma + p \rightarrow \Lambda^0 + K^+, \quad (2)$$

$$\gamma + p \rightarrow \Sigma^0 + K^+, \quad (3)$$

$$\gamma + n \rightarrow \Sigma^- + K^+. \quad (4)$$

The charge and lifetime of the  $K^+$  makes it feasible to use magnetic spectrometers to separate the kaons from the rather intense background arising from other photoprocesses.

The neutral kaon and short-lived hyperons limit the use of conventional techniques in reactions such as (1), (5), and (6).

$$\gamma + n \rightarrow \Lambda^0 + K^0, \quad (5)$$

$$\gamma + n \rightarrow \Sigma^0 + K^0. \quad (6)$$

<sup>†</sup> This work was supported by the National Science Foundation (Vanderbilt) and the U. S. Atomic Energy Commission (California Institute of Technology).

\* Present address: Department of Physics, University of Hawaii, Honolulu, Hawaii.

<sup>1</sup> C. E. Roos, E. Emery, and V. Z. Peterson, *Bull. Am. Phys. Soc.* **7**, 296 (1962).

<sup>2</sup> R. L. Anderson, E. Gabathuler, D. Jones, B. D. McDaniel, and A. J. Sadoff, *Phys. Rev. Letters* **9**, 131, (1962).

<sup>3</sup> F. Turkot, R. L. Anderson, D. A. Edwards, and W. M. Woodward, in *Proceedings of the Tenth Annual International Conference on High Energy Physics at Rochester, 1960* (Interscience Publishers, Inc., New York, 1960). This report on photo- $K^+$  reactions has references to most of the earlier work.

<sup>4</sup> R. L. Anderson, F. Turkot, and W. M. Woodward, *Phys. Rev.* **123**, 1003 (1961).

The forward laboratory angles of the kinematic cones for sigma photoproduction near threshold, combined with the low cross section and the short decay length have discouraged experimental studies. The maximum laboratory angle for a sigma produced by a 1.25-BeV photon is  $20^\circ$ . The electron shower background increases sharply at forward laboratory angles as seen in Fig. 1. If nuclear emulsions are simply placed at the required distances from a target exposed to a collimated 1.3-BeV bremsstrahlung beam they will be literally opaque at exposure intensities below that required for reasonable photosigma densities.

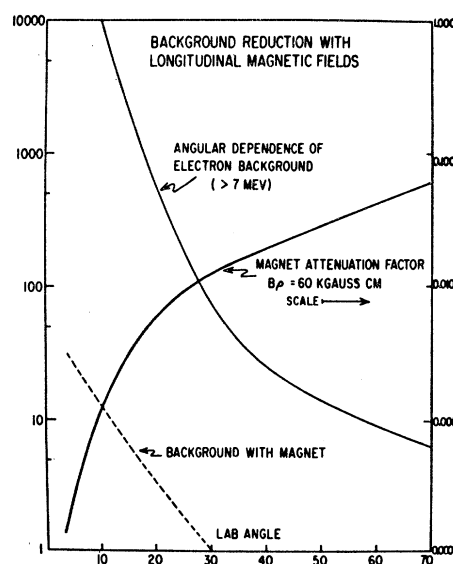


Fig. 1. Calculated shower electron background and magnet attenuation factor. The effect of the axial field is to reduce the charged background at a laboratory angle of  $10^\circ$  to the same level as the charged background at  $70^\circ$  without the use of the magnet. Electrons below 7 MeV are held by the field and cannot reach the emulsion at any angle.

It was realized that an intense axial magnetic field would focus the electron shower background along the photon beam axis. The transverse momentum component of the shower background is rarely larger than  $25 \text{ MeV}/c$  and a  $150\text{-kG}$  axial field will hold the charged component of the background to within  $4 \text{ mm}$  of the beam axis. The heavier charged hyperons have spiral paths of  $2\text{- to }3\text{-cm}$  radius and can still strike emulsion located just outside the region of shower containment.

The calculated reduction in the charged shower background, using a high-field magnet, is also shown in Fig. 1. The axial magnetic field is very effective at the forward angles where the electron shower background is greatest. While the actual improvement in sigma/shower background ratio will be limited by the Compton and shower photons, the charged shower background can be virtually eliminated. Experimental measurements<sup>5</sup> with lead targets and  $1.2\text{-BeV}$  bremsstrahlung confirm the calculations and demonstrate the effectiveness of  $160\text{-kG}$  axial fields in containing shower electrons.

#### EXPOSURE PROCEDURE

The design of the magnet, and the orientation of the emulsion stacks and target are shown in Fig. 2. The high-field magnet has been briefly described in review articles by one of the authors (VZP)<sup>6</sup> and by Fields.<sup>7</sup> The magnet was carefully designed for high magnetic efficiency. This reduces power dissipation in the magnet and permits rapid pulsing without extensive heating. Chilled oil was circulated through the magnet. While the  $1\frac{1}{2}\text{-in.}$  bore magnets have been tested up to  $250 \text{ kG}$ , the initial runs described in this communication were all made at  $160 \text{ kG}$ . At this field most of the electronic background is eliminated and the magnet was pulsed each  $10 \text{ sec}$  for thousands of pulses. The half-width of the magnet pulse is  $1.2 \text{ msec}$  while the beam of the Caltech electron synchrotron can be dumped in less than  $100 \mu\text{sec}$  at the time of peak field.

The turn density of the magnet varied with position such that the field was constant to  $2\%$  over a  $50\text{-cc}$  volume. Axial containment holds electrons originating from sources which are located in regions where the magnetic field is parallel to the beam axis. The target was placed in the region of constant field. Care was taken that the photon beam was swept free of charged particles prior to the  $\text{CH}_2$  target. The radial field components were as high as  $30 \text{ kG}$  at the ends of the  $160 \text{ kG}$  magnet, and this radial field can deflect the charged shower particles into the emulsions. Indeed the high-field magnet can actually increase the background in

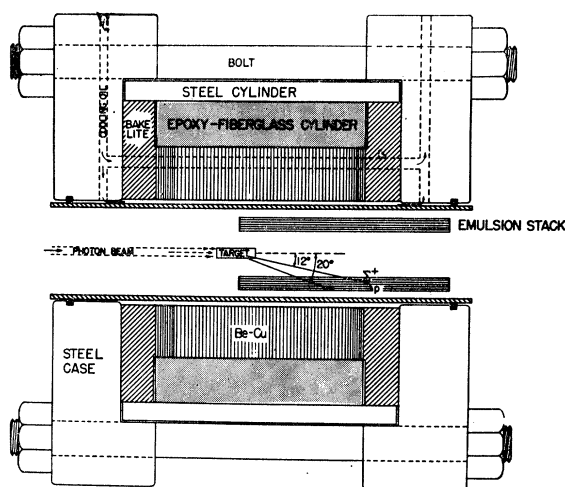


FIG. 2. High-field magnet, target, and emulsion orientation. The magnet coil is  $3\text{-in.}$  long and  $1\frac{1}{2}\text{-in.}$  i.d. The turn density is increased at the ends to maintain a more uniform field. The target region has less than a  $1\%$  radial component of the magnetic field.

the emulsion stacks if the photon beam is not free of charged particles.

Two stacks of Ilford K-5 ( $2\times$  dilute) emulsion were placed inside the high-field magnet, parallel to and  $6.5 \text{ mm}$  from the beam edge ( $8 \text{ mm}$  from center). A  $\text{CH}_2$  target ( $8 \text{ mm} \times 40 \text{ mm}$ )  $1.5\text{-gm}/\text{cm}^2$  thick was exposed to a total integrated bremsstrahlung energy of  $10^{13} \text{ MeV}$ , with a peak energy of  $1280 \text{ MeV}$ . The beam size at the target was  $3 \text{ mm}$  by  $10 \text{ mm}$ . One radiation length of LiH beam hardener was used to reduce the relative number of photons below  $25 \text{ MeV}$ . The beam path was evacuated after the beam hardener to eliminate interactions with the air. The charged particles from the beam hardener were removed by  $10 \text{ kG-m}$  of sweeping magnetic field. Considerable attention was paid to the alignment of collimators and scrapers, with the result that there was no detectable background in the absence of the target. The combination of careful collimation, beam hardening, sweeping magnets and axial field gave over two orders of magnitude of improvement in the sigma to background ratio. The plates examined for sigma decays showed very slight visual blackening and could be scanned for in-flight decays of twice minimum tracks.

#### PHOTOHYPERONS

The emulsion will detect the in-flight sigma decays as well as the charged decay mode of the  $\Lambda^0$ . The detection efficiency for light tracks limits the maximum detectable kinetic energy of the hyperons. The in-flight decay permits hyperon identification in spite of moderately heavy pion and proton backgrounds. Photohyperons produced near threshold are highly concentrated at forward laboratory angles. The scanned region

<sup>5</sup> A. D. McInturff and C. E. Roos, J. Tenn. Acad. Sci. 35, 108 (1960).

<sup>6</sup> V. Z. Peterson, in *Proceedings of the International Conference on High Magnetic Fields, 1961* (John Wiley & Sons Inc., New York, 1962), pp. 728-730.

<sup>7</sup> T. H. Fields, Nucl. Instr. Methods 20, 466 (1963).

TABLE I. Photohyperon events from CH<sub>2</sub>.

Event	Primary ionization at decay (G/G <sub>0</sub> )	Secondary ionization (G/G <sub>0</sub> )	Decay space angle (deg)	Target space angle (deg)	Target distance (cm)	Vertical displ. from beam (cm)	Energy at target (MeV)	Prob. for in-flight decay/cm	
								$\Sigma^+$	$\Sigma^-$
2- $\Sigma-\pi$	3.2	1.0	42	16.2	3.7	1.02	134	0.024	0.053
3- $\Sigma-\pi$	2.4	0.85	60	12.5	5.0	1.10	201	0.015	0.042
5- $\Sigma-\pi$	3.0	1.0	40	13.6	4.9	1.18	165	0.016	0.037
7- $\Sigma-\pi$	3.4	1.0	25	13.5	5.1	1.14	140	0.008	0.034
10- $\Sigma-\pi$	2.0	0.91	215	9.5	4.2	1.10	252	0.038	0.064
4- $\Sigma-p$	3.1	2.7	21	14.5	3.8	0.94	142	0.025	...
6- $\Sigma-p$	3.3	2.5	16	12.1	3.9	0.94	130	0.019	...
8- $\Sigma-p$	2.1	2.6	20	13.0	5.2	1.26	240	0.019	...
11- $\Sigma-p$	1.8	2.4	10	9.0	5.3	0.90	319	0.026	...
	proton	pion							
1- $\Lambda^0$	3.5	1.9	86	17	3.7	1.02	100	0.062	
2- $\Lambda^0$	4.1	3.0	38	15	4.0	1.02	50	0.039	

of the emulsion stack subtended a sigma c.m. solid angle of 1 sr.

The emulsions were area scanned. All events were required to have a minimum of 10% difference in grain density between primary and secondary tracks. This criterion eliminates elastic scatters but also excludes 25% of the valid proton mode  $\Sigma^+$  decays and 5% of the charged pion mode decays. In the scanned region, there were approximately 10 m of background tracks with ionization of less than 3.5 $\times$ minimum. These tracks might be expected to result in some 50 elastic and 30 inelastic events. The high  $Q$  value of the sigma results in a secondary with at least 10% less

ionization than the primary in approximately 45% of the proton mode decays and 95% of the pion mode decays. These events can be clearly distinguished from the background scatters and provide unambiguous identification of sigma decays. Approximately 30% of the proton mode decays have a proton track with more than 10% greater ionization than the sigma track. The kinematic requirements on energy and angle are quite severe and such events can be distinguished from inelastic scatters on a statistical basis.

All sigma tracks were traced to the second pellicle above the target. The pellicle next to the target was heavily exposed with low-energy tracks and was not used in the scanning. Scattering and grain counts were made along the length of the track. The ionization changes in the lower energy sigma events showed that these primaries came *from* the target. This reduces the possibility of confusing neutral stars with sigma decays. All secondaries which had more than minimum ionization were followed in the stack and grain counted. Typical ionization measurements on traced tracks were based on counts of at least 1000 grains. Minimum secondaries were grain counted but could not be traced to an adjacent pellicle with any reliability. A Leitz scattering microscope designed to measure scattering in depth was exceedingly useful in following the minimum tracks, and was used for analysis of all events. Both secondaries of the  $\Lambda^0$  decays were traced and grain counted. In one case the pion stopped in the emulsion.

The measured photohyperons are listed in Table I. Some "possible" events were not included because they were too light (1.3-1.5 $\times$ ) to trace and measure unambiguously. The first photosigma decay, shown in Fig. 3, was not included in Table I, since it was obtained in an earlier exposure using a carbon target. The sigma decay shown in Fig. 4 is event 2- $\Sigma-\pi$  in Table I. The pion track could be readily followed with a scattering microscope but is hard to identify in the presence

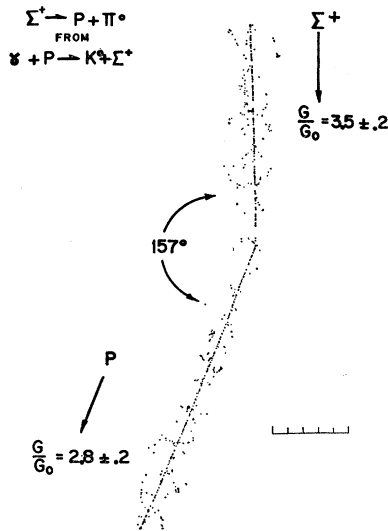


FIG. 3. Example of  $\Sigma^+ \rightarrow p + \pi^0$ . This event provided the first clear evidence of the reaction  $\gamma + p \rightarrow K^0 + \Sigma^+$ . It was obtained from a preliminary run with a carbon target and consequently is not included in Table I. The lighter secondary could not come from a scatter. The grain counts were each based on a minimum of 2000 grains. The primary was traced back and found to be coming from the target at a laboratory angle of 12° and with 125 MeV of kinetic energy.

of high minimum background. While not illustrated, the  $\Lambda^0$  decays were typical events.

The sigma kinetic energy at decay was obtained from the ionization measurements and this was corrected for energy loss in the emulsion stack and CH<sub>2</sub> target to obtain the energy at production. Two probabilities for in-flight decay/cm were calculated for the charged pion mode events, since they could be from either a  $\Sigma^+$  or  $\Sigma^-$ . The proton decays can only come from the  $\Sigma^+$ . The branching ratio is 50% and one should expect one pionic decay for each proton event.

There was no attempt to rescan the stack and directly measure the scanning efficiency for various types of hyperon decays. It is clear from Table I

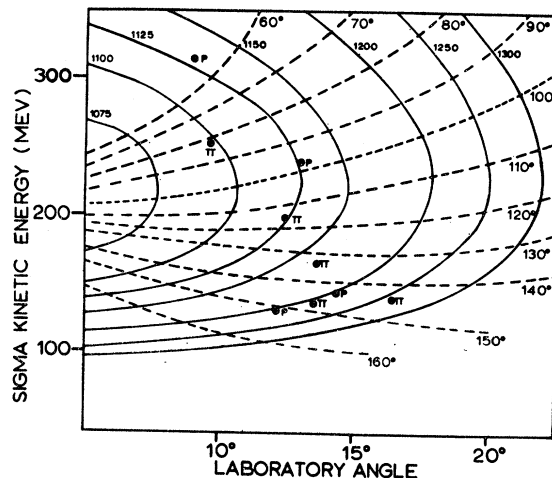


FIG. 5. Photosigma kinematic calculations assuming a stationary nucleon. The plotted events are the sigmas in Table I. The  $p$  indicates the proton and the  $\pi$  the charged pion made of decay.

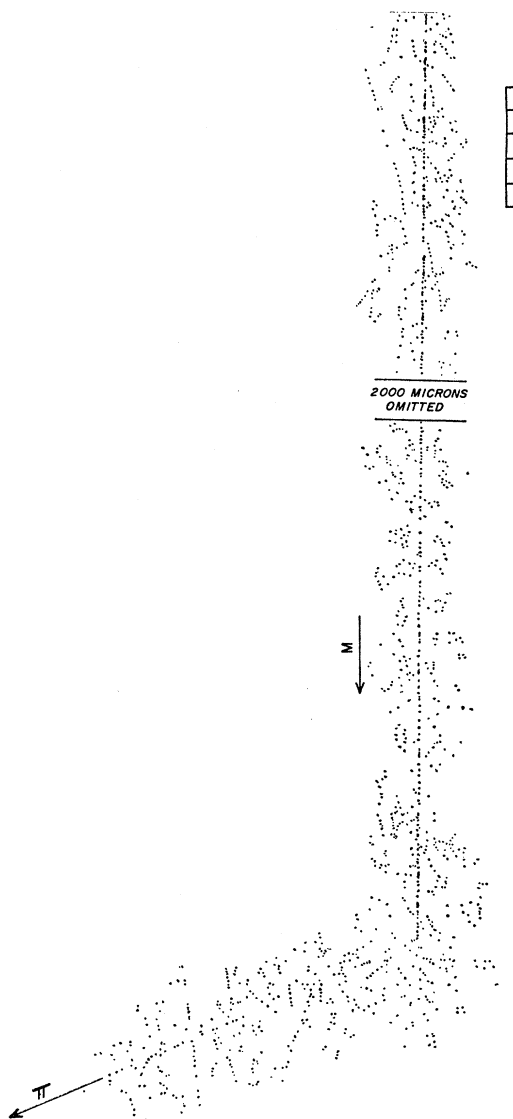


FIG. 4. Example of  $\Sigma^\pm \rightarrow \pi^\pm + n$ . The minimum secondary could be followed over several mm in the same plate. The primary ionization showed no significant change when traced to target.

that no event was seen that did not have one track darker than twice minimum. The pion events were all observed in pellicles high in the stack away from the beam where the background of minimum tracks was much reduced. The lower energy  $\Sigma^+$  proton decays are all found in pellicles close to the beam. Their short decay length sharply reduces the probability of finding them at greater distances from the target. The stack distribution suggests that the scanning efficiency for pion mode decays near the target and for events with ionizations of less than  $2x$  minimum was quite low.

#### DISCUSSION

The dependence of sigma kinetic energy on lab angle was calculated for hydrogen and is shown in Fig. 5 together with the events in Table I. With a CH<sub>2</sub> target the effects of nuclear motion prevent unambiguous identification of the c.m. angle and photon energy. The sigmas are seen to be most numerous at forward kaon angles. This may be due to scanning bias. Reactions (2) and (3) do have higher cross sections at forward kaon angles.<sup>2,3</sup>

A cross section for reaction (1) was calculated to be  $(4 \pm 2) \times 10^{-31}$  cm<sup>2</sup>/sr at a mean photon energy of 1.15 BeV and a mean sigma c.m. angle of 120°. Since no events without a  $2x$  minimum track were found the detection efficiency of such events was assumed to be zero, while for darker events it was assumed to be 100%. The above cross section may be a lower limit since it assumes that sigma production by the carbon protons is the same as that from hydrogen. There is no other data available on this reaction but it may be compared to the mean cross section<sup>2</sup> of  $(1.15 \pm 0.18) \times 10^{-31}$  cm<sup>2</sup>/sr at 1.16 BeV and 60° c.m. kaon angle found for reaction (3). The pion decay mode could

come from  $\Sigma^-$  produced from a neutron by reaction (4). The mean cross section of the observed values<sup>4</sup> is  $(0.9 \pm 0.4) \times 10^{-31}$  cm<sup>2</sup>/sr at 1.13 BeV and 79° c.m. kaon angle. If this value is assumed then we should have observed some three  $\Sigma^-$  decays in our stack. This suggests that about half of the  $\Sigma^\pm \rightarrow \pi^\pm + n$  decays were missed. This is quite reasonable in view of the difficulty of the scan and the observed distribution high in the stack of the pion mode decays. The cross section<sup>2,3</sup> for reaction (2) is  $(1.42 \pm 0.13) \times 10^{-31}$  cm<sup>2</sup>/sr at 90° cm and 1.13 BeV. This implies that only 30% of the detectable  $\Lambda^0$  decays were observed if reactions (5) and (6) have comparable cross sections. This is quite possible since sigma detection was given primary emphasis.

This paper reports the first measurement on reaction (1) and suggests that near threshold it has a higher cross section than either reactions (2) or (3). This difference is not surprising since different isotopic spin states can be involved.

Capps<sup>8</sup> has calculated ratios of the cross sections of the  $K-\Lambda$  and  $K-\Sigma$  charge states near threshold and found them quite sensitive to the  $K$ -hyperon parity using estimates of hyperon magnetic moments obtained from global symmetry.

At present new exposures with CH<sub>2</sub> are being scanned with substantially greater sigma densities and reduced background. With improved statistics it will be feasible to measure the  $\Sigma^+$  polarization. The asymmetry ratio is 1:4 for the five  $\Sigma-p$  events reported in this communication. A helium-cooled solid hydrogen

target<sup>9</sup> has already been developed and tested in the high-field magnet for use at the higher machine energies available in the near future. Increasing the maximum beam energy from 1280 to 1500 MeV will be of substantial benefit to this experiment since only photons above 1100 MeV produce  $\Sigma$ 's which decay in our emulsion, while most of the proton background comes from the lower energy photopion resonances.

#### ACKNOWLEDGMENTS

Numerous persons at the California Institute of Technology and at Vanderbilt assisted in this experiment. Professor R. F. Bacher has long supported the development of high-field magnets for use in conjunction with nuclear emulsion and he has encouraged this work. Dr. J. O. Maloy has contributed substantially to the development of the capacitor bank, firing circuits and related electronics. Dr. J. Teem helped in the early stages of this experiment. D. Lobbaka and E. Emery have worked on the high-field magnets and on the problems of beam alignment. The theoretical discussions and interest of Professor W. Holladay (V. U.) are gratefully acknowledged. A. D. McInturff (V. U.) assisted in the exposures at the California Institute of Technology, helped to develop the high field magnets, and worked on the photosigma background studies. Mrs. Carol Pridgen was in charge of the scanning laboratory (V. U.) and played a major role in the successful outcome of this experiment. William Monsarrat found four of the photohyperons.

<sup>8</sup> R. H. Capps, Phys. Rev. 114, 920 (1959).

<sup>9</sup> Constructed by A. D. McInturff.